

Okubo-Zweig-Iizuka rule violation in photoproduction

A. Sibirtsev¹, Ulf-G. Meißner^{1,2}, and A.W. Thomas³

¹*Helmholtz-Institut für Strahlen- und Kernphysik (Theorie),
Universität Bonn, Nußallee 14-16, D-53115 Bonn, Germany*

²*Institut für Kernphysik (Theorie), Forschungszentrum Jülich, D-52425 Jülich, Germany,*

³*Jefferson Lab, 12000 Jefferson Ave., Newport News, VA 23606, USA*

We investigate OZI rule violation in ω and ϕ -meson photoproduction off nucleons. Data on the total cross sections indicate a large ϕ/ω ratio of about 0.8 at the maximal available photon energy that is in good agreement with expectations from QCD. On the other hand, data at large four momentum transfer exhibit a ratio of about 0.07, showing that the perturbative QCD regime is not approached at $|t|>2$ GeV² and photon energies $E_\gamma<4$ GeV. The anomalously large ϕ/ω ratio at low energies, that is close to the reaction threshold, remains to be explained within nonperturbative QCD.

PACS numbers: 12.10.Kt; 12.38.Bx; 13.60.-r; 13.75.Cs; 13.75.Gx;

The violation of the OZI rule has been one of the more challenging aspects of QCD since the famous conjecture of Okubo, Zweig and Iizuka [1, 2, 3] based on the breaking of SU(3) symmetry. The ϕ -meson can be considered as a pure $s\bar{s}$ quark state if the octet and singlet mesons are ideally mixed with the angle $\theta_V=35.3^\circ$. Real life is not ideal and the experimental deviation from the ideal mixing angle is $\Delta\theta_V=3.7^\circ$ [4]. As a result, the ϕ -meson contains light quarks and the ratio of ϕ to ω -meson production in different reactions containing strange as well as non-strange quarks, such as $K^-p \rightarrow VY$, $\pi N \rightarrow VX$ or $NN \rightarrow VX$ ($V = \omega, \phi$), can be estimated [5] as $R_{\phi/\omega} = \tan^2 \Delta\theta_V \simeq 4.2 \times 10^{-3}$. The deviation of $R_{\phi/\omega}$ from zero in such reactions is usually referred to as OZI rule violation. One might expect an even larger ϕ/ω ratio from reactions involving nucleons because of the intrinsic $s\bar{s}$ content of the nucleon. In that case the strangeness component of the initial nucleon can be transferred to the final ϕ -meson. For a nice review on the OZI rule and its experimental tests, see [6].

A systematic analysis [7] of available data on ϕ and ω -meson production in pp and πp reactions gives $R_{\phi/\omega} \simeq (13.4 \pm 3.2) \times 10^{-3}$. This large ratio was interpreted [7] in terms pp and πp reaction dynamics that involves the $\phi\rho\pi$ and $\omega\rho\pi$ vertices. The $\phi\rho\pi$ coupling constant can be evaluated directly from the $\phi \rightarrow \rho\pi$ decay. The $\omega\rho\pi$ coupling can be extracted from $\omega \rightarrow 3\pi$ decay [8] or from $\omega \rightarrow \pi\gamma$ and $\rho \rightarrow \pi\gamma$ decays [9], that are dominated by the $\omega \rightarrow \rho\pi$ vertex with an intermediate vector meson coupled to the photon. The different decay modes provide [7] an average ratio of $R_{\phi/\omega} \simeq (12.5 \pm 3.4) \times 10^{-3}$, which is in a good agreement with available results from pp and πp reactions. It is clear that the large experimental ϕ/ω ratio is dictated by the large $\phi \rightarrow \rho\pi$ decay width and is not related to the strangeness content of the nucleon. It is well known [10] that the $\phi \rightarrow \rho\pi$ decay violates the OZI rule. We remark that new experiments with the ANKE detector at COSY [11] and at the JINR Nuclotron [12] are devoted to the investigation of OZI rule violation at energies close to the $pp \rightarrow pp\phi$ reaction threshold. Here, we present the current status of OZI

rule violation in vector meson photoproduction from nucleons.

The solid squares and circles in Fig.1a) show the available experimental results on the total cross section for ω and ϕ -meson photoproduction off a proton as a function of photon energy [13, 14, 15, 16]. The triangles in Fig.1a) are the most recent results on ϕ -meson photoproduction at $E_\gamma < 2.6$ GeV measured at ELSA [17], while the open circles show ELSA results for ω -photoproduction [18]. The solid lines indicate calculations based on the pomeron exchange model [19, 20],

$$\frac{d\sigma}{dt} = \frac{81m_V^2\beta_0^4\mu_0^4\Gamma}{\pi\alpha} \left[\frac{s}{s_0} \right]^{2\alpha_P(t)-2} \times \frac{F^2(t)}{(m_V^2 - t)^2(2\mu_0^2 + m_V^2 - t)^2}, \quad (1)$$

where t and s are the four-momentum transfer and the invariant collision energy squared, respectively, m_V is the mass of the vector meson V , Γ is the $V \rightarrow e^+e^-$ decay width, α is the fine-structure constant and $F(t)$ is the proton isoscalar electromagnetic form factor, approximated as

$$F(t) = \frac{4m_p^2 - 2.8t}{4m_p^2 - t} \frac{1}{(1 - t/t_0)^2}. \quad (2)$$

Here, m_p is the proton mass and $t_0=0.7$ GeV². The free parameters of the model are related to the pomeron-quark vertex, namely the coupling constant, β_0 , and the cut-off of the form factor, μ_0 . The pomeron trajectory $\alpha_P(t)$ is given by [21]

$$\alpha_P(t) = \alpha_0 + \alpha't, \quad (3)$$

where $\alpha_0=1.008$ and $\alpha'=0.25$ GeV⁻². The constant $s_0=1/\alpha'$ was determined utilizing the dual model prescription [22]. The parameter $\mu_0^2=1.1$ GeV was evaluated [19, 21] from high energy data on elastic and inelastic scatterings at small $|t|$. A systematic analysis [16] of total and differential cross sections for ω -meson photoproduction results in $\beta_0=2.35$ GeV⁻¹. Fig.1a) illustrates

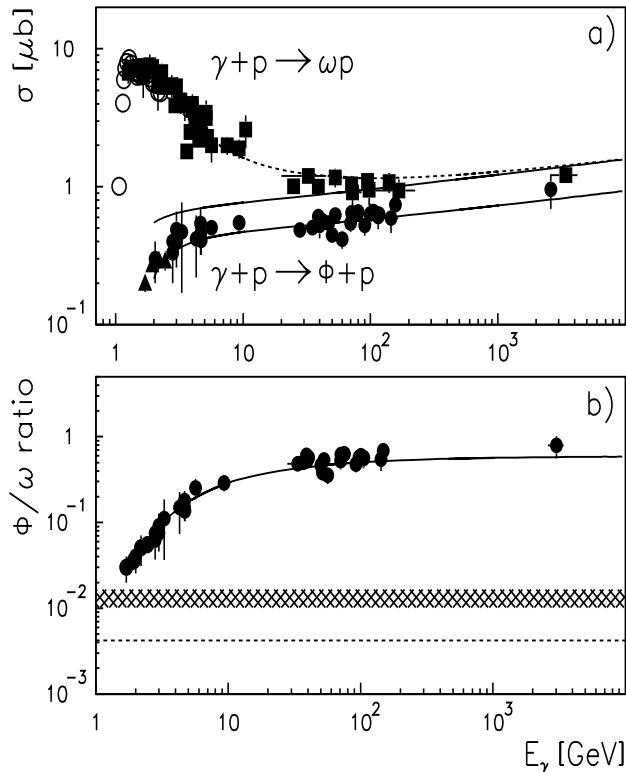


FIG. 1: a) Total cross section for exclusive ω and ϕ photoproduction off the proton as a function of the photon energy. The solid squares and circles show the data collected in Refs. [13, 14, 15, 16]. The triangles and open circles show most recent results from ELSA [17, 18] for ϕ and ω -meson photoproduction respectively. The solid lines give the result from pomeron exchange, while the dashed line shows the calculations for the ω -meson with both meson and pomeron exchange contributions. b) The ratio $R_{\phi/\omega}$. The dashed line is the ratio given by SU(3) mixing, the shaded area indicates results from πp and pp reactions and the solid line is the ratio of the calculations presented in a).

that pomeron exchange describes the data on ω -meson photoproduction at photon energies above 100 GeV quite well. To reproduce the data at lower energies it is necessary to account [16] for both meson exchange and pomeron contributions – as shown by the dashed line in Fig.1a). To reproduce the total cross section for ϕ -meson photoproduction we readjust $\beta_0=1.9 \text{ GeV}^{-1}$. The pomeron exchange alone describes the total cross section of the $\gamma p \rightarrow \phi p$ reaction even at low energies.

In Fig. 1b) we display the data on the ratio of ϕ to ω total photoproduction cross sections together with the calculations presented in Fig.1a). The dashed line in Fig.1b) is the ratio $R_{\phi/\omega}=4.2 \times 10^{-3}$, given by the octet and singlet mixing, while the shaded strip shows the result from πp and pp reactions. Apparently the OZI rule is strongly violated in photoproduction. At high energies the interaction is driven by gluon exchange and is flavor-blind. Thus we would expect that in the perturbative QCD regime the ϕ/ω ratio might ap-

proach unity up to the corrections associated with the hadronic wave functions of the ω and ϕ -mesons. Indeed the data collected in Fig.1b) show that $R_{\phi/\omega} \simeq 0.5$ and that it does not depend on the photon energy at $30 \leq E_\gamma < 200 \text{ GeV}$. At the maximal available photon energy $R_{\phi/\omega} \simeq 0.8 \pm 0.2$. This result is in reasonable agreement with the non-perturbative QCD quark-pomeron interaction that should also be flavor-blind. Although we found that in reality the quark-pomeron coupling depends on the quark flavor and $\beta_0=2.35, 1.9$ and 0.45 GeV^{-1} for light, strange and charm [20] quarks, respectively, the data on the large ϕ/ω ratio support the dominance of QCD interactions at high energies.

Furthermore, the photoproduction data indicate a large ratio $R_{\phi/\omega} > 0.03$ even at threshold. The agreement between the ϕ -meson photoproduction data and pomeron calculations at low energies does not provide a reasonable explanation of the large ratio. It is known that the pomeron theory is applicable [21] in the high energy region, $E_\gamma > 10 \text{ GeV}$, and an agreement between the data and calculations at low energies might be rather accidental. For instance, a systematic analysis [20, 23] of J/Ψ -photoproduction also indicates good agreement between the total photoproduction cross section and pomeron exchange at threshold, but at the same time shows a strong disagreement between the calculated and the measured J/Ψ -meson differential spectra. Apparently a systematic analysis of ϕ -meson photoproduction is necessary to understand the reaction mechanism and the anomalously large ratio $R_{\phi/\omega}$ at low energies.

It is important that the QCD regime be studied at high energies and at large four momentum transfer squared. At large $|t|$ the interaction probes small distances $\simeq 1/\sqrt{-t}$ and can be described by multi-gluon exchange and constituent quark interchange [24, 25, 26]. Because of the OZI rule, quark interchange does not contribute to ϕ -meson photoproduction and one might expect that the $\gamma p \rightarrow \phi p$ reaction at large $|t|$ would be dominated by gluon exchange. Indeed, the two-gluon exchange model [27, 28] reproduces data on ϕ -meson photoproduction at large $|t|$. On the contrary, ω -photoproduction allows for quark interchange. This might result in a small value for $R_{\phi/\omega}$. If both ω and ϕ -meson photoproduction are dominated by gluon exchange, we might expect a large $R_{\phi/\omega}$, compatible with the result shown in Fig.1b) at high photon energies. It is worthwhile to note the analogy between the phenomenological pomeron and two-gluon exchange [19, 29], which allows for explicit comparison of large $|t|$ and high energy data.

High accuracy data on ω and ϕ -meson photoproduction at large $|t|$ were collected by the CLAS Collaboration at JLab [30, 31] and are shown in Fig.2 and Fig.3a). The solid lines in Fig.2 show the calculation based on meson and nucleon exchange, with vertex parameters fixed by data available prior to the CLAS measurements. Here the ω -meson photoproduction at large $|t|$ is dominated by the nucleon exchange current, while at low $|t|$ the dom-

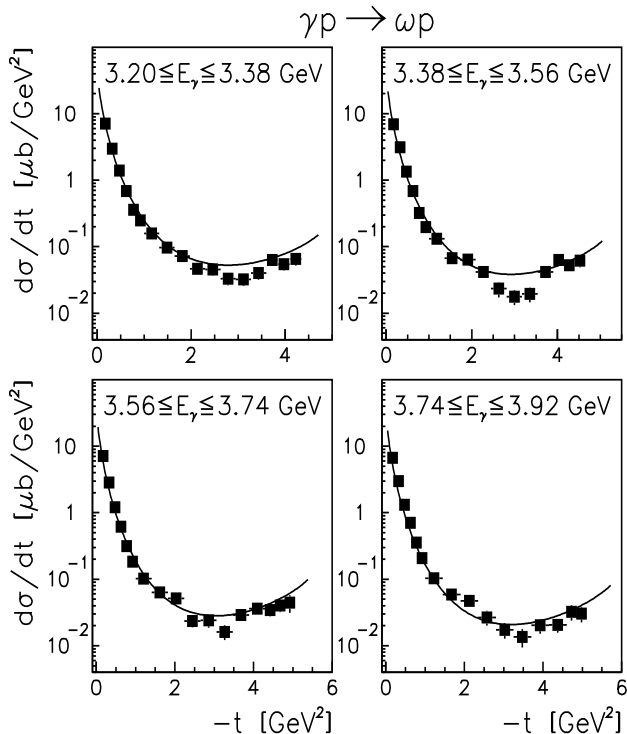


FIG. 2: Differential cross section for $\gamma p \rightarrow \omega p$ reaction as a function of four momentum transfer squared [31]. The lines show the meson and nucleon exchange calculations [32].

inant contribution comes from π and σ -exchange. The solid line in Fig.3a) represents the calculations based on pomeron exchange utilizing Eq.(1). Fig.3b) shows the ϕ/ω ratio as a function of $|t|$.

Let us first discuss the result at low $|t|$ where $R_{\phi/\omega} \simeq 0.15$. As we mentioned before, the application of the pomeron exchange at low energies can not be justified theoretically [16, 20, 21] and one might consider the contribution from π and σ -exchange, as in ω -meson photoproduction. In that case the ϕ/ω ratio depends on the ratio of the $\phi\pi\gamma$ and $\omega\pi\gamma$ coupling constants squared, which is $\simeq (3.5 \pm 0.2) 10^{-3}$ [9, 10], close to the ratio given by SU(3) mixing. We would not expect σ -exchange to contribute much more to ϕ -meson photoproduction in comparison to ω -photoproduction. At least this is not supported by estimates given by $\phi \rightarrow \pi\pi\gamma$ and $\omega \rightarrow \pi\pi\gamma$ decays [4]. The η -exchange also plays a minor role [32].

Therefore either one would accept that pomeron exchange already dominates ϕ -photoproduction at threshold or we must consider another possible nonperturbative mechanism. For instance near threshold J/Ψ -meson photoproduction was discussed in terms of three gluons [33] or anomalous axial exchange [23]. While neither mechanism depends strongly on the photon energy, they have a very different low $|t|$ dependence, which can be used for an experimental falsification of such models. For illustration we show in Fig. 4 the exponential slope of the t -dependence for exclusive ω and ϕ -meson photoproduction. The solid lines indicate the slope fit-

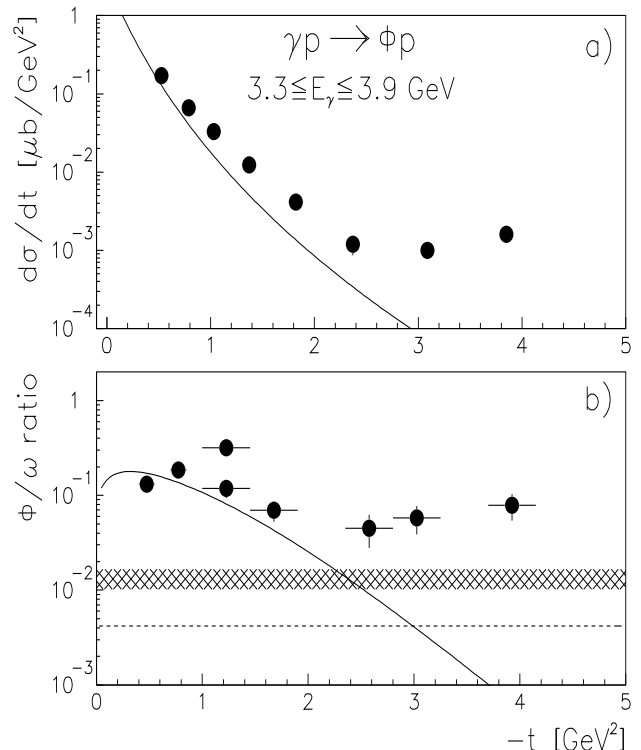


FIG. 3: a) Differential cross section for the $\gamma p \rightarrow \phi p$ reaction as a function of four-momentum transfer squared [30]. The solid lines represent the calculations based on pomeron exchange. b) The ϕ/ω ratio as function of $-t$. The dashed line is the ratio given by SU(3) mixing, the shaded area indicates the results from πp and pp reactions and the solid line is the ratio of the calculations with meson and nucleon exchanges in the ω case and with pomeron exchange for ϕ -photoproduction.

ted to pomeron exchange calculations at $|t| < 0.6$ GeV². At low energies the slope of $\gamma p \rightarrow \phi p$ data differs from the pomeron calculation where the minimal slope is driven by the proton isoscalar electromagnetic form factor squared [20]. The data indicate a soft contribution with a slope around 4 GeV⁻² at energies $E_\gamma < 10$ GeV. The open circles and triangles in Fig. 4 shows most recent high precision results from ELSA [17, 18] for ω and ϕ -photoproduction, respectively. The ELSA data apparently indicate a small slope and are inconsistent with pomeron exchange. Moreover the ELSA ϕ -meson photoproduction measurements [17] of the spin density matrix elements clearly contradicts the expectations based on the pomeron model. However, apart from the ELSA measurements, the data at $E_\gamma < 10$ GeV are not sufficiently accurate to draw more solid conclusions. In that respect, new precise differential cross section data from ELSA, JLab and SPRING8 on ϕ -meson photoproduction are of great importance.

Furthermore the ϕ/ω ratio at large $|t|$, $R_{\phi/\omega} \simeq 0.07 \pm 0.01$, differs substantially from that at high energies, which is in disagreement with the two-gluon exchange model. Other nonperturbative mechanisms, such as (for example) multi-gluon exchange

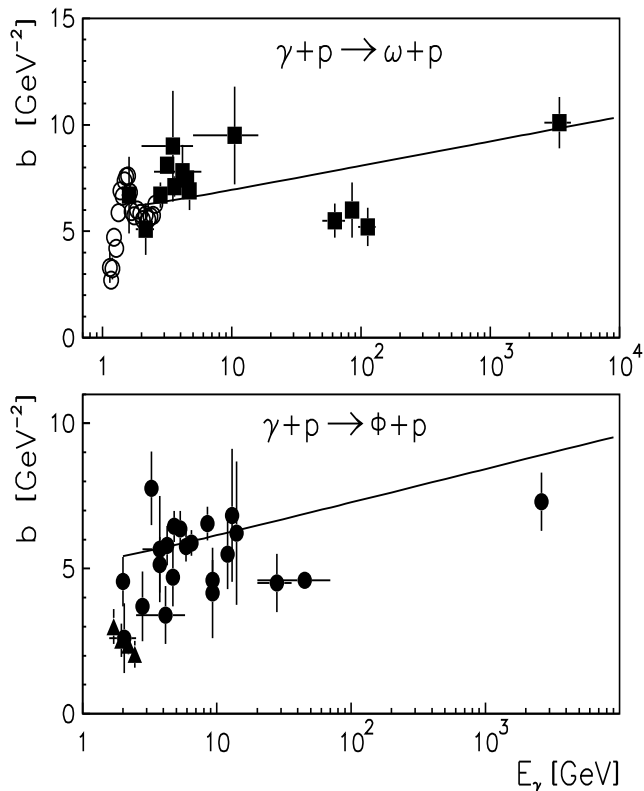


FIG. 4: Exponential slope of the t -dependence for exclusive ω and ϕ -photoproduction as a function of the photon energy. Solid squares and circles show the data collected in Refs. [14, 16, 34, 35, 36, 37, 38]. The open circles and triangles indicate recent results measured at ELSA [17, 18] for ω and ϕ -meson photoproduction, respectively. Solid lines show the result of the pomeron exchange model.

are also not supported by the data, since any flavour-blind interaction would result in a large ratio close to the $R_{\phi/\omega} \simeq 0.5$ observed at high energies in the QCD regime.

Alternatively one might consider nucleon exchange, which has been shown to contribute to ω -photoproduction at large- $|t|$, as illustrated by Fig. 2 and might also contribute to ϕ -meson photoproduction. In that case the ϕ/ω ratio at the same t would be given explicitly by the ratio of the ϕpp and ωpp coupling constants squared. Modern dispersion theoretical analysis [39, 40] of the nucleon electromagnetic form factors shows that the squared ratio of the ϕpp to ωpp vector couplings is $\simeq 0.23$. The dispersion analysis is based on a maximal violation of the OZI rule because the isoscalar spectral function in the mass region above 1 GeV was taken to come entirely from the ϕ -pole. The combined analysis [41] of the results from the nucleon-nucleon interaction and nucleon electromagnetic form factors led to a substantially smaller ratio, of order 5.3×10^{-4} . The analysis [42, 43] of the angular ϕ -meson spectra from the pp interaction provides an upper limit of the squared ratio as $\simeq 0.024$. Obviously within these large

uncertainties of the ratio for the ϕpp and ωpp couplings one might describe ϕ -meson photoproduction at large $|t|$ by nucleon exchange.

To summarize, we have given a systematic analysis of OZI rule violation in vector meson photoproduction. The data on the total cross sections for ϕ and ω -meson photoproduction indicate a ratio $R_{\phi/\omega} \simeq 0.8 \pm 0.2$ at the maximal available photon energy. This large ratio is in agreement with pomeron or two-gluon exchange calculations and fulfills QCD expectations at high energies. Moreover, we found that the ϕ/ω ratio is already greater than 0.03 at threshold – that is, it substantially exceeds the ratio $R_{\phi/\omega} = 4.2 \times 10^{-3}$ expected from SU(3) mixing. At low photon energies this anomalously large ratio can be explained if one assumes that the ϕ -meson production is already entirely dominated by pomeron exchange at threshold.

On the other hand, the available data at large four-momentum transfer squared indicate that the QCD regime is not approached at $|t| > 2 \text{ GeV}^2$ and $E_\gamma < 4 \text{ GeV}$. Here the ratio $R_{\phi/\omega} \simeq 0.07 \pm 0.01$ differs from the results observed at high energies. We speculate that at low photon energies and large $|t|$ the ϕ/ω ratio might be explained by the nucleon exchange mechanism. At low $|t|$ the ratio approaches $\simeq 0.15$ and can once again be understood in terms of the dominance of pomeron or two-gluon exchange in ϕ -meson photoproduction at low photon energies. However, such a dominance is in contradiction with results available for the exponential slope of the t -dependence, which indicate a soft component at low- $|t|$ photoproduction at $E_\gamma < 10 \text{ GeV}$. The soft component rules out the pomeron exchange model at low energies because of the coupling of the pomeron to the isoscalar electromagnetic form factor of the proton, which results in a large slope [20].

In conclusion, while all available data for ω and ϕ -meson photoproduction explicitly indicate a substantial violation of the OZI rule and show a ϕ/ω ratio much larger than that obtained [7] from πp and pp reactions, only part of our findings can be explained in terms of perturbative QCD. The large ϕ/ω ratio at low energies remains a puzzle of nonperturbative QCD, see also [44]. Further progress apparently requires new, precise data on ϕ -meson photoproduction close to the reaction threshold, as well as intensive theoretical activity to develop new QCD methods at low energies.

Acknowledgments

We appreciate discussions with M. Battaglieri, J. Haidenbauer, C. Hanhart, M. Hartmann, F. Klein and S. Krewald. This work was partially supported by the Department of Energy under contract DE-AC05-84ER40150 under which SURA operates Jefferson Lab, by Deutsche Forschungsgemeinschaft through funds provided to the SFB/TR 16 “Subnuclear Structure of Matter” and by the COSY FFE grant No. 41445400 (COSY-067). This research is part of the EU Integrated Infrastructure Initiative Hadron Physics Project under con-

tract number RII3-CT-2004-506078.

-
- [1] S. Okubo, Phys. Lett. **5**, 165 (1963).
 [2] G. Zweig, CERN report TH-401 (1964).
 [3] J. Iizuka, Prog. Theor. Phys. Suppl. **38**, 21 (1966).
 [4] Particle Data Group, Phys. Lett. B **592**, 1 (2004).
 [5] H.J. Lipkin, Phys. Rev. Lett. B **60**, 371 (1976).
 [6] V. P. Nomokonov and M. G. Sapozhnikov, Phys. Part. Nucl. **34**, 94 (2003) [Fiz. Elem. Chast. Atom. Yadra **34**, 189 (2003)] [arXiv:hep-ph/0204259].
 [7] A. Sibirtsev and W. Cassing, Eur. Phys. J. A **7**, 407 (2000) [nucl-th/9907059].
 [8] M. Gell-Mann and F. Zachariasen, Phys. Rev. **124**, 953 (1961).
 [9] U.-G. Meißner, Phys. Rep. **161**, 213 (1988).
 [10] P. Jain, R. Johnson, U.-G. Meißner, W. Park and J. Schechter, Phys. Rev. D **37**, 3252 (1988).
 [11] M. Hartmann *et al.* Proc. BARYONS 2004, to be publ. in Nucl. Phys. **A**.
 [12] R.A. Salmin *et al.*, Proc. Hadron Structure 2002, 280 (2002).
 [13] J. Busenitz *et al.*, Phys. Rev. D **40**, 1 (1989).
 [14] M. Derrick *et al.*, Phys. Lett. B **377**, 259 (1996) [hep-ex/9601009].
 [15] Landolt-Börnstein, New Series **I/12**, Springer (1998).
 [16] A. Sibirtsev, K. Tsushima and S. Krewald, Phys. Rev. C **67**, 055201 (2003) [nucl-th/0301015].
 [17] J. Barth *et al.*, Eur. Phys. J. A **17**, 269 (2003).
 [18] J. Barth *et al.*, Eur. Phys. J. A **18**, 117 (2003).
 [19] A. Donnachie and P.V. Landshoff, Nucl. Phys. B **311**, 509 (1988).
 [20] A. Sibirtsev, S. Krewald and A.W. Thomas, J. Phys. G **30**, 1427 (2004) [nucl-th/0301082].
 [21] A. Donnachie and P.V. Landshoff, Phys. Lett. B **296**, 227 (1992) [hep-ph/9209205].
 [22] G. Veneziano, Nuov. Cim. A **57**, 190 (1968).
 [23] A. Sibirtsev, S. Krewald and A.W. Thomas, nucl-th/0310021.
 [24] J.F. Gunion, S.J. Brodsky and R. Blankenbecler, Phys. Lett. B **39**, 649 (1972).
 [25] P.V. Landshoff and J.C. Polkinghorne, Phys. Rev. D **8**, 927 (1973).
 [26] S.J. Brodsky and G.R. Farrar, Phys. Rev. D **11**, 1309 (1975).
 [27] A. Donnachie and P.V. Landshoff, Phys. Lett. B **185**, 403 (1987).
 [28] J.M. Laget and R. Mendez-Galain, Nucl. Phys. A **185**, 397 (1995).
 [29] J.R. Cudell, Nucl. Phys. B **336**, 509 (1990).
 [30] E. Anciant *et al.*, Phys. Rev. Lett. **85**, 4682 (2000) [hep-ex/0006022].
 [31] M. Battaglieri *et al.*, Phys. Rev. Lett. **90**, 022002 (2003) [hep-ex/0210023].
 [32] A. Sibirtsev, K. Tsushima and S. Krewald, AIP Conf. Proc. **717**, 280 (2004); nucl-th/0202083.
 [33] S.J. Brodsky, E. Chudakov, P. Hoyer and J.M. Laget, Phys. Lett. B **498**, 23 (2001) [hep-ph/0010343].
 [34] R. Erbe *et al.*, Phys. Rev. **175**, 1669 (1969).
 [35] J. Ballam *et al.*, Phys. Rev. D **7**, 3150 (1973).
 [36] H.J. Behrend *et al.*, Nucl. Phys. B **144**, 22 (1978).
 [37] D. Aston *et al.*, Nucl. Phys. B **172**, 1 (1980).
 [38] M. Atkinson *et al.*, Z. Phys. C **27**, 233 (1985).
 [39] H.W. Hammer and U.-G. Meißner, Eur. Phys. J. A **20**, 469 (2004) [hep-ph/0312081].
 [40] P. Mergell, U.-G. Meißner and D. Drechsel, Nucl. Phys. A **596**, 367 (1996) [hep-ph/9506375].
 [41] U.-G. Meißner, V. Mull, J. Speth and J.W. van Orden, Phys. Lett. B **408** 381 (1997), [hep-ph/9701296].
 [42] J. Haidenbauer, K. Nakayama, J.W. Durso, C. Hanhart and J. Speth, Proc. Baryons 98 (1988) [nucl-th/9810069].
 [43] K. Nakayama, J.W. Durso, J. Haidenbauer, C. Hanhart and J. Speth, Phys. Rev. C **60**, 055209 (1999) [nucl-th/9904040].
 [44] N.I. Kochelev and V. Vento Phys. Lett. B **515**, 375 (2001) [hep-ph/0104070]; Phys. Lett. B **541**, 281 (2002) [hep-ph/0110268].